Noise Reduction in Brain Magnetic Resonance Imaging Using a Convolutional Autoencoder

I Gede Susrama Mas Diyasa[1*], Pangestu Sandya Etniko Siagian[2], Eva Yulia Puspaningrum[3], Wan Suryani Wan Awang[4], Sayyidah Humairah[5], and Deshinta Arrova Dewi[6]
[1]Department of Master in Information Technology, Faculty of Computer Science, University of Pembangunan Nasional "Veteran" Jawa Timur Surabaya, Indonesia 60294
[2,3]Department of Informatics, Faculty of Computer Science, University of Pembangunan Nasional "Veteran" Jawa Timur Surabaya, Indonesia 60294
[4]Department of Computer Science, Faculty of Informatics and Computing, University Sultan Zainal Abidin Besut Campus Terengganu, Malaysia 21300
[5]Department of Electrical and Computer Engineering, Polytechnic Faculty, University of Patras Rio, Greece 26504
[6]Center for Data Science and Sustainable Technologies, INTI International University Negeri Sembilan, Malaysia 71800
Email: [1]igsusrama.if@upnjatim.ac.id, [2]21081010180@student.upnjatim.ac.id, [3]evapuspaningrum.if@upnjatim.ac.id, [4]suryani@unisza.edu.my, [5]humairahs@upatras.gr, [6]deshinta.ad@newinti.edu.my

***Abstract*—In clinical practice, precise and high-quality brain Magnetic Resonance Imaging (MRI) is pivotal for diagnosing and formulating effective treatment strategies. The research objective is to assess the viability of employing a Convolutional Autoencoder (CAE) for mitigating noise in brain MRI images. The focus is on brain MRI images and the various types of noise (Salt and Pepper, Speckle, and Gaussian noise) that typically corrupt images and may lead to inaccuracies in diagnosis. The research also applies methods to artificially generate these noise types to represent real-world scenarios. Specifically, the dataset of brain MRI images is collected, pre-processed, and artificially exposed to various noise types to simulate the real-world conditions after the CAE model is used to reconstruct the corrupted images. The CAE is assessed for its high efficiency and efficacy using Mean Squared Error (MSE) and Peak Signal-to-Noise Ratio (PSNR). The results indicate that the CAE is very effective in removing noise, particularly Salt and Pepper noise. The model achieves a PSNR of 27.0687 dB and an MSE of 0.00216246 at the lowest noise level. The model also demonstrates stability under varying levels of Speckle noise. Although performance degrades as noise increases, the model continues to demonstrate potential for further refinement. The research furthers the CAE's analytical potential by assessing its denoising capabilities across various noise types and levels. The research adds value by outlining recommendations to the medical imaging community while identifying the need for future research on different classifications of noise and advanced regularization methods.**

***Index Terms*—Convolutional Autoencoder (CAE), Cancer, Magnetic Resonance Imaging (MRI) Denoising, Noise Reduction, Deep Learning, Image Enhancement, Process Innovation**

I. Introduction

MAGNETIC Resonance Imaging (MRI) is one of the most widely used non-invasive diagnostic imaging modalities in modern clinical medicine. Unlike Computed Tomography (CT) or conventional X-ray imaging, MRI does not expose patients to ionizing radiation and provides superior soft-tissue contrast, making it particularly valuable for neurological examinations. Given its critical role in diagnosis and treatment planning, the quality of brain MRI images must be maintained at the highest possible standard,

Received: March 03, 2025; received in revised form: July 01, 2025; accepted: July 03, 2025; available online: April 02, 2026.
*Corresponding Author

as even minor image degradation can adversely affect clinical decision-making [1, 2].

Despite advances in MRI technology, acquired images are frequently degraded by noise arising from scanner hardware limitations, patient motion, and environmental interference. Conventional noise reduction methods, such as Gaussian, Median, and Wiener filters, often fail to preserve the fine structural details critical for accurate medical interpretation [3]. The emergence of deep learning, particularly Convolutional Neural Networks (CNNs) and their autoencoder variants, has provided a more effective approach by learning complex mappings between noisy and clean images directly from data, motivating its application in MRI denoising tasks [4, 5].

In conducting research, a comprehensive review of previous research is essential to build a solid theoretical foundation and framework. Previous study has examined five different contrast enhancement algorithms, including Histogram Equalization, which is a global method, and Adaptive Histogram Equalization, which performs local contrast enhancement. The performance of these algorithms is evaluated using standard measures such as Root Mean Square Error (RMSE), Peak Signal to Noise Ratio (PSNR), and Tenengrad Measure (TGD) [6].

Another study has conducted a comparative analysis of various filtering techniques for brain MRI noise reduction, including Wiener, Median, and Gaussian filters. Their findings reveal important limitations in conventional filtering approaches. While certain filters, such as the Median filter, demonstrates effectiveness in reducing specific types of noise (particularly Salt and Pepper noise), its performance is not consistently optimal across all noise scenarios. Although the Median filter outperforms the Average filter under specific conditions, it shows limitations in completely eliminating Speckle noise [3].

To improve image quality, a previous study has developed an adaptive Non-Local Means (NLM) filter in which a bilateral filter is used to pre-enhance the MRI images, followed by multi-resolution wavelet domain processing to remove coefficients containing more noise than signal. It accounts for the Rician nature of MRI noise distribution and demonstrates significant improvement over standalone methods such as Gaussian smoothing, Wiener filter, and wavelet thresholding [7]. In a related study, an improved adaptive Wiener filter is proposed that identifies the noise type based on its histogram distribution, calculates the mean and variance of the noise, and constructs a corresponding point spread function to estimate the adaptive Signal-to-Noise Ratio (SNR) of the image. This approach directly determines the optimal SNR for the Wiener filter without continuous SNR estimation required by the traditional Wiener filter, achieving superior denoising performance in terms of PSNR [8]. In assessing the effectiveness of denoising methods such as those above, the SNR, PSNR, and Mean Squared Error (MSE) metrics are commonly used [7, 8].

A significant advancement in denoising techniques is introduced in a study proposed by RicianNets, a Convolutional Neural Network architecture implementing a progressive learning strategy for MRI image denoising. This novel approach demonstrates superior performance metrics, achieving a higher PSNR of 28.1 dB and Structural Similarity Index (SSIM) of 0.7480 compared to conventional denoising methods. It marks a significant improvement in the field [4].

Previous research has further developed the area by using Convolutional Autoencoder (CAE) to denoise medical images, particularly X-ray and CT scans. It demonstrates strong evidence of CAE's applicability, especially in cases of limited medical image datasets. It has studied the use of CAE model to achieve noise reduction in X-ray and CT images and examined the effects of various types of noise, including Gaussian, Salt and Pepper, and Speckle noise across varying degrees of noise. The CAE proves in achieving noise reduction and demonstrates strong performance in medical image feature extraction, with an average PSNR of 31.66098 X-ray images and 30.4040 dB of CT Scan images, respectively. On average, it also reports a SSIM of 0.8715 for X-ray and 0.8698 for CT Scan images [5].

Drawing from past studies and techniques, the current research seeks to establish the potential use of the CAE model for noise reduction in medical images by training the model to restore original images from noise-affected images. CAE is chosen due to its relative advantage over commonly applied linear filtering techniques. In particular, it better retains and restores critical detailed patterns prevalent in medical images. MRI images of the brain must be of the highest possible quality, and even the slightest noise can jeopardize reliable diagnoses and clinical decision-making [1, 2].

The central research problem in this research is how effectively a CAE can remove various types of noise in brain MRIs while maintaining image quality . The research attempts to deepen the understanding of the application of deep learning in the enhancement of medical imaging and the potential incorporation of Artificial Intelligence (AI) in the medical imaging diagnosis process. The focus is on evaluating the denoising ability of the CAE for brain MRIs with noise types including Salt noise, Pepper noise, Salt and Pepper noise, and Speckle noise. Their performance is evaluated using MSE and PSNR.

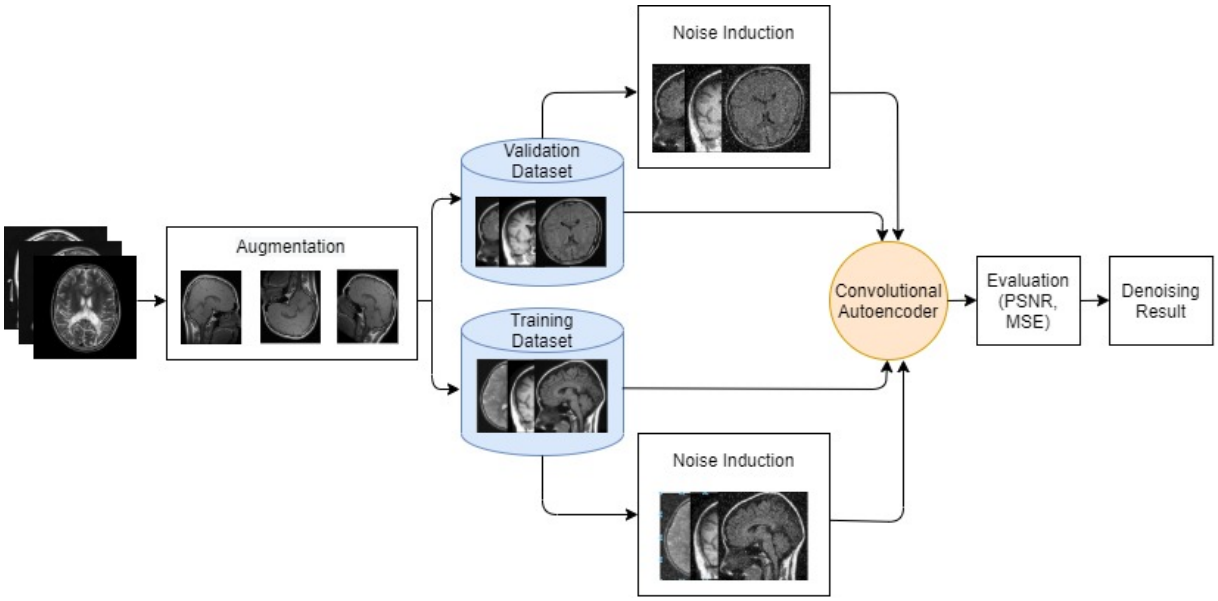

Fig. 1. Methodological workflow. Note: Mean Squared Error (MSE) and Peak Signal-to-Noise Ratio (PSNR).

II. Research Method

The research adopts a methodical approach that aims to promote organization and facilitate problem-solving during the investigation. The research methodology serves as a comprehensive guideline, directing the study from its initial stages through to completion. Each methodological phase has been carefully designed to maintain a clear research structure while effectively addressing the established research objectives and problem statements. As shown in Fig. 1, the complete workflow includes data collection, image preprocessing, noise induction, model training, and result evaluation. The goal is to develop a model that is able to improve the quality of MRI images by removing noise, so that they can be used for further medical analysis [9, 10].

A. Data Collection

The initial phase involves collecting brain MRI images from the Kaggle dataset called "Crystal Clean: Brain Tumors MRI Dataset." This dataset consists of two main categories: normal brain MRI images and brain MRI images with tumors. However, the research only utilizes normal brain MRI images. This dataset contains three types of human head orientations. The basic MRI planes are side to side (sagittal plane), front to back (coronal plane), and top to bottom (axial plane) [11–13], as shown in Fig. 2. It presents a sample from the MRI dataset. For model training, 2,082 normal brain MRI images are collected as training data. In addition, to evaluate the performance of the model,

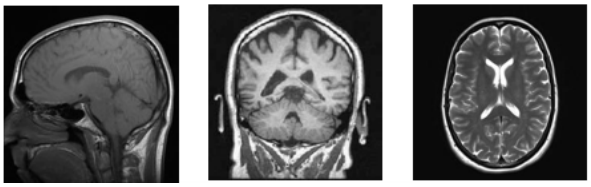

Fig. 2. Sample of brain Magnetic Resonance Imaging (MRI) dataset.

522 normal brain MRI images are used as validation data. The MRI images used have the format ".jpg." This stage is crucial as it establishes the foundation for subsequent analysis and model development. The quality and diversity of the acquired images directly influence the model's learning capabilities and performance [14–16].

B. Pre-Processing

The pre-processing phase for the MRI images obtained from the Kaggle dataset involves several standardization steps to ensure optimal data quality for model training [17]. The process begins with dataset quality control. It is implemented to ensure data integrity. Images with severe artifacts or corruption are identified and removed. Poor quality images that can potentially impact model training that are also filtered out [15, 18, 19]. The next step involves resolution standardization, in which all images are scaled to a uniform dimension of 256×256 pixels. Following the resolution standardization, the images undergo grayscale conversion.

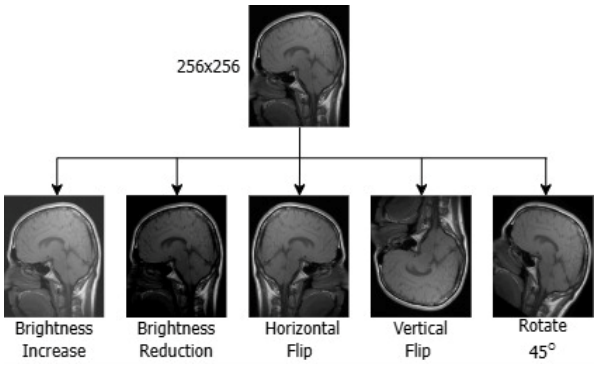

Fig. 3. Sample of data augmentation techniques applied to brain Magnetic Resonance Imaging (MRI) images.

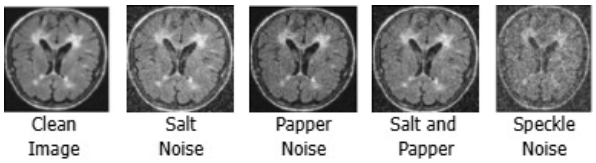

Fig. 4. Sample of noise types artificially induced on brain Magnetic Resonance Imaging (MRI) images.

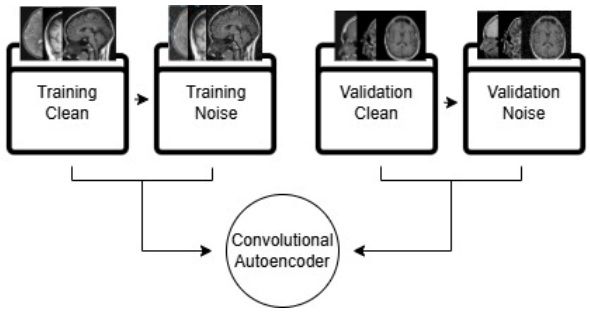

Fig. 5. Sample of clean and noisy brain Magnetic Resonance Imaging (MRI) image pairs used in the training and validation pipeline of the Convolutional Autoencoder (CAE) model.

Data augmentation is a crucial step in this research to enhance the variability of the training data without the need to collect additional data. This process is carried out by modifying brain MRI images using various augmentation techniques, allowing the model to handle diverse variations in input data. The augmentation aims to improve the model's generalization by simulating real-world conditions with varying characteristics [20, 21]. Some of the augmentation techniques employed include brightness adjustment, darkness adjustment, horizontal/vertical flipping, and rotation, as shown in Fig. 3 [21–23].

These techniques help to mitigate overfitting and maintain optimal performance of the model across various applications. Additional training using transformed data helps the model to learn the core attributes of the data, irrespective of perceptual variations caused by noise. This technique improves the model's performance and further reduces the risk of overfitting [24]. As a result, the model can handle more intricate and varied inputs with greater accuracy.

For the research, the dataset of 2,604 normal brain MRI images is divided into an 80:20 ratio. A total of 80% of the data (2,082 images) is used as the training set, enabling the model to learn patterns and features from the input data. The remaining (20% of the dataset (522 images)) is used as the validation set. This set is used to assess the model's performance during training and to gauge the model's ability to generalize to novel data [25].

C. Noise Induction

At this stage, the brain MRI images used as training and validation data are intentionally subjected to noise to simulate conditions. MRI data may be affected by disturbances, resulting in artifacts [5]. Due to the difficulty of obtaining MRI images with inherent noise, artificial noise is added to generate noisy versions of the images, enabling the model to learn how to remove such noise [26–28]. The types of noise introduced include Salt noise, Pepper noise, Salt and Pepper noise, and Speckle noise as shown in Fig. 4. These different noise patterns mimic actual distortions in the image acquisition process, presenting a realistic challenge for a model to address [29–31].

This phase produces two data sets. The first one has clean training data and noisy training data. The second one has clean validation data and noisy validation data. Each subset is fed to the model to the train the model on effective denoising [32, 33]. This way, the model learns to work with both clean and dirty images. Hence, it improves the generalization of the model in varying conditions, as demonstrated in Fig. 5.

D. Proposed Model

The first stage of the Kaggle dataset of MRI image preprocessing consists of multiple standardization procedures carried out to ensure that the data have the highest possible quality prior to model training. This process began with dataset quality control to ensure data integrity. Images with severe artifacts or corruption are identified and removed. Poor quality images that can potentially impact model training are also filtered out. The next step involves resolution standardization, in which all images are scaled to a uniform dimension of 256×256 pixels, as illustrated in Fig. 6.

The encoder consists of three convolutional layers, each followed by Batch Normalization and MaxPool-

Cite this article as: I. G. S. M. Diyasa, P. S. E. Siagian, E. Y. Puspaningrum, W. S. W. Awang, S. Humairah, and D. A. Dewi, "Noise reduction in brain magnetic resonance imaging using a convolutional autoencoder", CommIT Journal 20(1), 115–125, 2026.

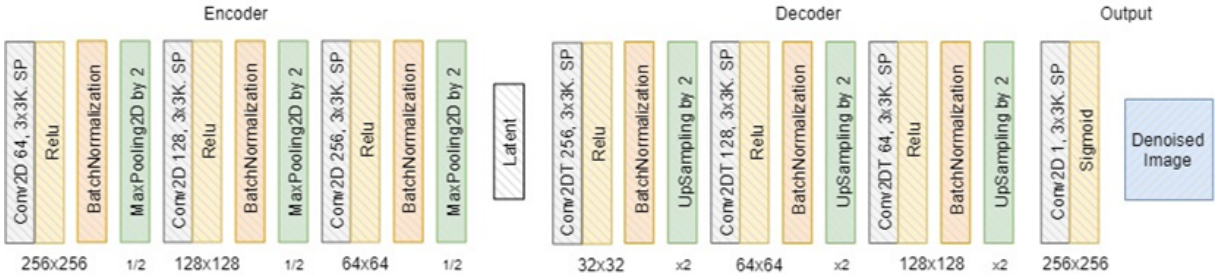

Fig. 6. Architecture of the proposed Convolutional Autoencoder (CAE) model, illustrating the encoder pathway from 256×256 to 32×32 and the decoder pathway from 32×32 back to 256×256, along with the corresponding layer configurations.

ing to reduce spatial dimensionality while extracting higher-level features. The first layer uses 64 filters, the second layer uses 128 filters, and the third layer uses 256 filters, each with a 3×3 kernel and "same" padding to preserve spatial resolution. After passing through the encoder, the representation is compressed through MaxPooling operations. The decoder then reconstructs the image by applying transposed convolutional layers (also known as deconvolution), progressively upsampling the feature maps to recover the original image dimensionality. Batch Normalization is applied after each transposed convolutional layer to stabilize training, and the final layer produces a reconstructed image with one channel using a sigmoid activation function for pixel values between 0 and 1 as illustrated in Fig. 6. The model is compiled using the Adam optimizer with MSE as the loss function.

E. Experiment Setup

MSE is applied as a loss function because the main goal is to reduce the difference between the recovered image and the original image. MSE quantifies the differences between original and reconstructed pixel values. A small batch size, such as 8, improves data handling, reduces overfitting, and helps to prevent memory limitation during training. At the same time, a small number of epochs (15) is selected to allow quick assessment of the model performance without prolonged training time. The ADAM optimizer is used due to its adaptive learning rate capabilities. Proper hyperparameter optimization can improve the stability of the CAE model during training [34].

The CAE model is tested with four different types of noise (Speckle noise, Salt noise, Pepper noise, and Salt and Pepper noise) as shown in Table I. Each type of noise is applied to the MRI images, and each method is tested with three different parameter values: 0.05, 0.10, and 0.15. In the context of Salt, Pepper, and Salt and Pepper noise, these variance values indicate the proportion of pixels affected by noise corruption,

TABLE I
TESTING SCENARIO.

Parameter	Value
Noise	Salt, Pepper, Salt and Pepper, Speckle
Variance	0.05, 0.1, 0.15
Evaluation	Mean Squared Error (MSE), Peak Signal-to-Noise Ratio (PSNR)

ranging from 5% to 15% of the total image pixels. For Speckle noise, these parameters represent the intensity of multiplicative noise applied to the original image, where higher values indicate greater deviation from the original pixel values [5]. The model then learns to reconstruct clean images from the noisy inputs. The quality of the model's reconstruction results was measured using two metrics, MSE and PSNR, for each type of noise.

Equation (1) is used to measure the average difference between two images, namely the original image and the reconstructed (or degraded) image. The calculation is performed by computing the difference between each pixel of the two images and squaring the difference to eliminate negative values and magnify the impact of larger differences. After that, all the squared differences are summed and divided by the total number of pixels in the image (calculated by multiplying the height and width of the image in pixels) to obtain the mean squared error value. The smaller the MSE value is, the smaller the difference between the original image and the reconstructed image will be. It indicates that the reconstructed image has better quality. Equation 1 has w as the width of the image, representing the total number of pixels in the horizontal direction, h as the height of the image, representing the total number of pixels in the vertical direction, i as the pixel index in the horizontal direction, ranging from 0 to $w-1$, j as the pixel index in the vertical direction, ranging from 0 to $h-1$, $I(i,j)$ as the pixel intensity value of the original (clean/reference) image at position (i,j), and $K(i,j)$ as the pixel intensity value of the

reconstructed (denoised) image produced by the CAE at position (i, j).

$$MSE = \frac{1}{w \times h} \sum_{i=0}^{w-1} \sum_{j=0}^{h-1} (I(i,j) - K(i,j))^2 \quad (1)$$

PSNR measures the ratio between the maximum strength of a signal (in this case, the original image) and the strength of the noise corruption that affects the fidelity of its representation. A higher PSNR value indicates better image quality, as it reflects lower distortion compared to the original image [35, 36]. The PSNR is an important metric for evaluating image quality. The formula for the PSNR is given in Eq. 2. This metric helps evaluate how well the model removes different types of noise, thereby identifying the strengths and weaknesses of CAE in handling specific noise types.

$$PSNR = 10 \times \log_{10} \frac{255^2}{MSE} \quad (2)$$

III. Results and Discussion

The analysis provides insights regarding the behavior of the CAE model under various types and levels of noise. The use of different noise types and intensity reveals clear distinctions in the training and validation loss curves. In the research, four types of noise (Salt, Pepper, combined Salt and Pepper, and Speckle noise) are employed at three levels of intensity (0.05, 0.1, and 0.15) to evaluate the model's learning process and generalization ability, as shown in Fig. 7.

Loss curves for Salt noise in the CAE model show clear convergence, and for all levels of noise, the training loss decreases significantly in the initial iteration, after which the validation loss follows the training loss. In this case, effective generalization is observed without signs of underfitting. The highest convergence stability is observed in the validation loss curves at the highest level of noise intensity (0.15).

Figure 7 illustrates the loss curves for Pepper noise, which demonstrate the most complicated learning dynamics over time. While the noise loss during training shows a consistent decrease, the loss associated with validation exhibits significant oscillations, especially during later epochs. This behavior is indicative of the model's inability to generalize for this noise type. The greater the divergence is between training and validation loss, especially at noise intensity columns 0.1 and 0.15, the more potential there is for further optimizations through increased regularization and adjustments to the training procedure.

The combined Salt and Pepper noise loss curves in Fig. 7 show the most stable learning progression. The training and validation losses exhibit consistent patterns of convergence, regardless of the noise intensity, and the curves show little divergence. This result suggests that the model architecture is suited for this specific type of combined noise and has generalized well during the training process.

Figure 7 suggests that the loss curves for Speckle noise show some temporally varying patterns during the learning process. Initial epochs show rapid convergence in both training and validation losses, followed by a gradual refinement phase. Minor oscillations in validation loss during later epochs, coupled with continuing decreases in training loss, suggest potential benefits from implementing adaptive learning rate strategies for optimization in extended training scenarios.

The quantitative evaluation of the model's denoising performance reveals distinct patterns across different noise types and intensities. The evaluation incorporates two dimensions: PSNR, expressed in decibels (dB) and MSE. Both of them provide a complementary view of the model's efficacy, as illustrated in Table II.

The performance of the CAE model in the presence of Salt noise is revealed by the PSNR values of 26.2640 dB at 0.05 noise intensity and 25.4988 dB at 0.15 noise intensity. MSE values of 0.00258830 and 0.00296704 also indicate a very small increase, signifying that the reconstruction quality remains consistent, despite an increase in the noise intensity. A small degradation in reconstruction quality, even as the noise level increases, denotes that the model has sufficient noise suppression capability for this type of noise.

Table II in the row for 'Pepper' shows the model having the highest dispersion in performance across different levels of noise. The PSNR values show a drop of 3.6069 dB, from 23.9652 dB at noise intensity 0.05 to 20.3585 dB at noise intensity 0.15. Meanwhile, the MSE shows a significant increase from 0.00455104 to 0.01098814. The model clearly has increasing trouble with higher intensities when reconstructing images corrupted with Pepper noise.

The CAE model provides the greatest overall performance with combined Salt and Pepper noise, as illustrated in Table II. PSNR values start at 27.0687 dB for 0.05 intensity and remains close at 25.5662 dB for 0.15 intensity. The MSE values exhibits a modest increase from 0.00216246 to 0.00296106, demonstrating the model's ability to reduce noise despite the presence of various combined noise types. The model's architecture appears to excel with this common type of image corruption, leading to its outstanding performance.

Speckle noise performance exhibits noteworthy uniformity in the management of speckle noise across various levels in intensity, as detailed in Table II. The PSNR measurements show a range between 25.6936

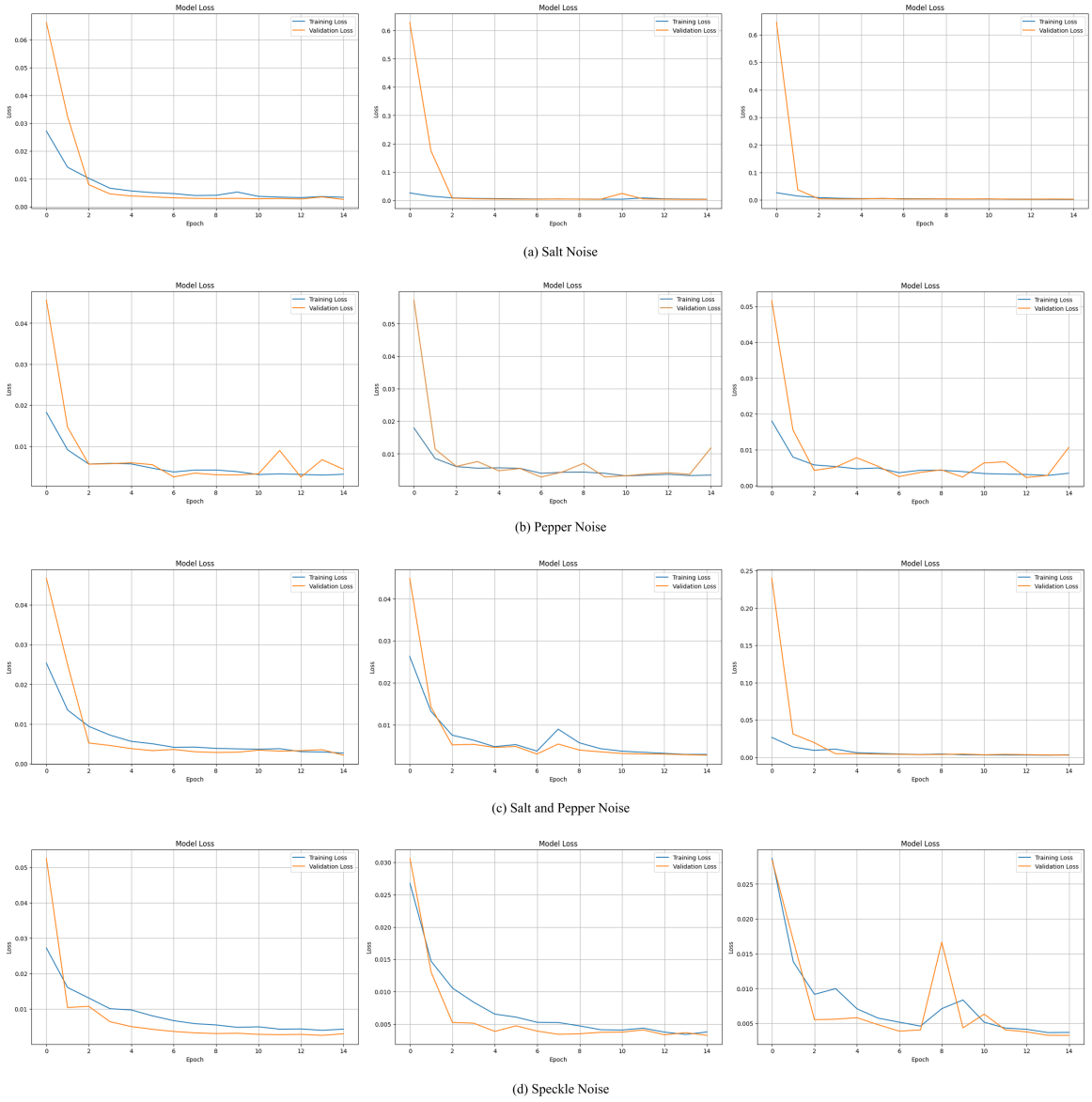

Fig. 7. Training and validation loss curves of the Convolutional Autoencoder (CAE) model across four noise types at three intensity levels (variance = 0.05, 0.10, and 0.15): (a) Salt noise, (b) Pepper noise, (c) Salt and Pepper noise, and (d) Speckle noise. Each row presents three subplots corresponding to increasing noise intensity from left to right.

TABLE II
RESULTS OF DENOISING PERFORMANCE.

Noise Type	Peak Signal-to-Noise Ratio (PSNR)			Mean Squared Error (MSE)		
	0.05	0.1	0.15	0.05	0.1	0.15
Salt	26.2640 dB	25.1797 dB	25.4988 dB	0.00258830	0.00302152	0.00296704
Pepper	23.9652 dB	22.9569 dB	20.3585 dB	0.00455104	0.00550253	0.01098814
Salt and Pepper	27.0687 dB	25.8912 dB	25.5662 dB	0.00216246	0.00280482	0.00296106
Speckle	25.6936 dB	25.2701 dB	25.1722 dB	0.00302918	0.00322526	0.00326723

dB and 25.1722 dB, and the MSE demonstrates slight variation between 0.00302918 and 0.00326723. This consistency across multiple performance metrics demonstrates the stability and effectiveness of the

model in handling multiplicative noise, especially for medical imaging applications.

The average PSNR for the model is 27.0687 dB for reconstruction quality of Salt and Pepper noise at 0.05, which is the best measured Salt and Pepper quality. It is recorded for the Salt and Pepper noise type and noise intensity with a low level of MSE of 0.00216246, confirming the model's capability at low noise intensity with a low level of noise intensity. Generally better PSNR values are above 30 dB. Accurate data are of utmost importance because the higher the data is the better. The 20–30 dB range may present a further target. A lower target range is 0–20 dB. Blurring may occur at lower PSNR values [37, 38].

Speckle noise processing exhibits the least amount of inconsistency across the different ranges of intensities as evidenced by the small variations in MSE and PSNR measurements. This stability suggests that the model's architecture is particularly well-suited for handling multiplicative noise patterns, a characteristic that is especially valuable in medical imaging applications where consistent performance is crucial. The consistent performance at increasing noise levels suggests this noise type is suitable for feature extraction and reconstruction.

Processing Pepper noise has proven to be the most problematic for the denoising model, especially at more intense levels. The model's architecture may need targeted alterations to more effectively manage isolated dark-pixel noise patterns, as indicated by the steep drop in PSNR values and the concomitant rise in MSE at 0.15 intensity. This commentary provides a basis for future architectural advancements and dedicated preprocessing approaches to address greater intensity pepper noise in medical imaging.

IV. Conclusions

The research demonstrates the effectiveness of the CAE architecture in denoising brain MRI images across various noise types and intensities. The model shows particularly strong performance in handling combined Salt and Pepper noise, achieving the highest PSNR of 27.0687 dB and lowest MSE of 0.00216246 at 0.05 intensity. The architecture shows notable stability in processing Speckle noise across all intensity levels, indicating effective handling of multiplicative noise patterns. However, the model faces challenges with isolated pepper noise at higher intensities, suggesting room for optimization.

The research has a number of limitations. First, the computational limitations are due to the hardware specifications of the author's laptop (an ASUS TUF FA506QM laptop with an AMD Ryzen 7-5800H CPU, an NVIDIA GeForce RTX 3060 GPU, and 16GB of RAM). It constrains the author's ability to perform hyperparameter tuning and to train more complex model architectures. Second, the dataset used is limited to brain MRIs acquired from a Kaggle dataset, which may have limited the model's ability to generalize across different images and protocols. Finally, the current architecture does not include many regularization layers, which may have decreased the model's ability to generalize across different types of noise.

Many potential areas for future research have been recognized. First, engineering improvements to the architecture may be possible by adding more regularization layers to enhance the generalization and stability of the models. Second, the investigation can be expanded to include other prevalent noise types in medical imaging, particularly Poisson noise (Shot noise) and Periodic noise, which are not addressed in the current study. Future work should also explore more sophisticated hyperparameter optimization strategies, contingent upon access to more powerful computational resources. While clinical implementation is not within the scope of the research, future research can investigate the practical application of these denoising techniques in clinical settings, including real-time processing capabilities and integration with existing medical imaging workflows.

Acknowledgement

The authors would like to express their sincere gratitude to the Institute for Research and Community Service (LPPM) of UPN "Veteran" Jawa Timur for the institutional support and research facilitation provided throughout this study. Appreciation is also extended to the Center for Data Science and Sustainable Technologies, INTI International University, Malaysia, for their academic collaboration, constructive insights, and support in strengthening the scientific quality of this research. The support from both institutions has significantly contributed to the successful completion of this study.

Author Contribution

Conceived and designed the analysis, I. G. S. M. D.; Contributed data or analysis tools, I. G. S. M. D.; Constructed and supervised the model architecture and experimental framework, I. G. S. M. D.; Collected the data, P. S. E. S.; Performed data preprocessing, augmentation, and noise induction, P. S. E. S.; Constructed and performed the model experiment, P. S. E. S.; Created the experiment design and validation strategy, E. Y. P.; Wrote the introduction and research method, E. Y. P.; Performed validation and analysis

of training–validation loss, W. S. W. A.; Gave advice about model performance and optimization, W. S. W. A.; Wrote the experiment result, S. H.; Prepared tables and visualizations, S. H.; Critically reviewed and edited the manuscript, D. A. D.; and Gave advice about scientific contribution and publication readiness, D. A. D.

Data Availability

The data that support the findings of the research are openly available in Kaggle at https://www.kaggle.com/datasets/mohammadhossein77/brain-tumors-dataset.

References

[1] W. Y. Leong, "AI-generated brain scans for synthetic healthcare data," in *2025 21st IEEE International Colloquium on Signal Processing & Its Applications (CSPA)*. Pulau Pinang, Malaysia: IEEE, Feb. 7–8, 2025, pp. 140–143.

[2] R. K. Manoj, A. N. S., and M. Batumalay, "Automated brain tumor analysis with multimodal fusion and augmented intelligence," *Journal of Applied Data Sciences*, vol. 6, no. 2, pp. 1277–1290, 2025.

[3] J. Shedbalkar, K. Prabhushetty, and A. Inchalc, "A comparative analysis of filters for noise reduction and smoothening of brain MRI images," in *2021 6th International Conference for Convergence in Technology (I2CT)*. Maharashtra, India: IEEE, April 2–4, 2021, pp. 1–6.

[4] S. Li, J. Zhou, D. Liang, and Q. Liu, "MRI denoising using progressively distribution-based neural network," *Magnetic Resonance Imaging*, vol. 71, pp. 55–68, 2020.

[5] W. El-Shafai, S. Abd El-Nabi, E. S. M. El-Rabaie, A. M. Ali, N. F. Soliman, A. D. Algarni, and F. E. Abd El-Samie, "Efficient deep-learning-based autoencoder denoising approach for medical image diagnosis," *Computers, Materials, & Continua*, vol. 70, no. 3, pp. 6107–6125, 2022.

[6] K. Srinivasan and N. Muthu, "A comparative study and analysis of contrast enhancement algorithms for MRI brain image sequences," in *2018 9th International Conference on Computing, Communication and Networking Technologies (ICCCNT)*. Bengaluru, India: IEEE, July 10–12, 2018, pp. 1–7.

[7] K. Kagoiya and E. Mwangi, "A hybrid and adaptive non-local means wavelet based MRI denoising method with bilateral filter enhancement," *International Journal of Computer Applications*, vol. 166, no. 10, pp. 1–7, 2017.

[8] Q. Zhang, C. Liu, and G. He, "An improved wiener filter based on adaptive SNR MRI image denoising algorithm," in *2022 International Conference on Computing, Communication, Perception and Quantum Technology (CCPQT)*. Xiamen, China: IEEE, Aug. 5–7, 2022, pp. 164–168.

[9] Z. Li, Z. Li, H. Li, Q. Fan, K. L. Miller, W. Wu, A. S. Chaudhari, and Q. Tian, "Enhance the image: Super resolution using artificial intelligence in MRI," 2024. [Online]. Available: http://arxiv.org/abs/2406.13625

[10] A. G. Cicimen, H. F. J. Tregidgo, M. Figini, E. Messaritaki, C. B. McNabb, M. Palombo, C. J. Evans, M. Cercignani, D. K. Jones, and D. C. Alexander, "Image quality transfer of diffusion MRI guided by high-resolution structural MRI," in *International Workshop on Computational Diffusion MRI*. Marrakesh, Morocco: Springer, Oct. 6, 2024, pp. 106–118.

[11] T. Vyas, R. Yadav, C. Solanki, R. Darji, S. Desai, and S. Tanwar, "Deep learning-based scheme to diagnose Parkinson's disease," *Expert Systems*, vol. 39, no. 3, 2022.

[12] F. Bertacchini, R. Rizzo, E. Bilotta, P. Pantano, A. Luca, A. Mazzuca, A. Lopez, and Alzheimer's Disease Neuroimaging Initiative, "Mid-sagittal plane detection for advanced physiological measurements in brain scans," *Physiological Measurement*, vol. 40, no. 11, 2019.

[13] W. Krois, F. Palmisani, P. Gröpel, P. Feil, M. L. Metzelder, J. M. Patsch, and C. A. Reck-Burneo, "Assessment of sacral ratio in patients with anorectal malformations: Can magnetic resonance imaging replace conventional radiograph?" *Journal of Pediatric Surgery*, vol. 56, no. 11, pp. 1993–1997, 2021.

[14] J. Kugelman, D. Alonso-Caneiro, S. A. Read, S. J. Vincent, F. K. Chen, and M. J. Collins, "Effect of altered OCT image quality on deep learning boundary segmentation," *IEEE Access*, vol. 8, pp. 43 537–43 553, 2020.

[15] V. Kamath, A. Renuka, V. G. Kini, and S. Prabhu, "Exploratory data preparation and model training process for Raspberry Pi-based object detection model deployments," *IEEE Access*, vol. 12, pp. 45 423–45 441, 2024.

[16] M. Böhland, R. Bruch, S. Bäuerle, L. Rettenberger, and M. Reischl, "Improving generative adversarial networks for patch-based unpaired image-to-image translation," *IEEE Access*, vol. 11, pp. 127 895–127 906, 2023.

[17] I. G. S. M. Diyasa, V. I. Sunarko, E. Y. Puspaningrum, V. Asy'ari, and M. Z. Ibrahim, "Op-

timization of multi-section and partially augmented Magnetic Resonance Imaging (MRI) images for brain tumor classification using ResNet-50," *CommIT (Communication and Information Technology) Journal*, vol. 19, no. 1, pp. 115–128, 2025.

[18] E. Delamare, X. Fu, Z. Huang, and J. Kim, "Panoramic imaging errors in machine learning model development: A systematic review," *Dentomaxillofacial Radiology*, vol. 53, no. 3, pp. 165–172, 2024.

[19] I. G. S. M. Diyasa, B. Damanik, and M. R. Mahendra A., "Classification of pneumonia using a deep learning convolutional neural network," in *2023 IEEE 9th Information Technology International Seminar (ITIS)*. Batu Malang, Indonesia: IEEE, Oct.18–20, 2023, pp. 1–5.

[20] H. Alsaif, R. Guesmi, B. M. Alshammari, T. Hamrouni, T. Guesmi, A. Alzamil, and L. Belguesmi, "A novel data augmentation-based brain tumor detection using convolutional neural network," *Applied Sciences*, vol. 12, no. 8, pp. 1–16, 2022.

[21] A. S. Chauhan, J. Singh, S. Kumar, N. Saxena, M. Gupta, and P. Verma, "Design and assessment of improved convolutional neural network based brain tumor segmentation and classification system," *Journal of Integrated Science and Technology*, vol. 12, no. 4, pp. 793–793, 2024.

[22] I. Kandel, M. Castelli, and L. Manzoni, "Brightness as an augmentation technique for image classification," *Emerging Science Journal*, vol. 6, no. 4, pp. 881–892, 2022.

[23] E. H. Fuadi, A. R. Ruslim, P. W. K. Wardhana, and N. Yudistira, "Gated self-supervised learning for improving supervised learning," in *2024 IEEE Conference on Artificial Intelligence (CAI)*. Singapore: IEEE, June 25–27, 2024, pp. 611–615.

[24] A. Biswas and M. S. Islam, "A hybrid deep CNN-SVM approach for brain tumor classification," *Journal of Information Systems Engineering & Business Intelligence*, vol. 9, no. 1, pp. 1–15, 2023.

[25] M. P. J. Van Der Loo and E. De Jonge, "Data validation," in *Wiley StatsRef: Statistics reference online*. Wiley, 2020.

[26] I. Nagarajan and G. G. Lakshmi Priya, "Removal of noise in MRI images using a block difference-based filtering approach," *International Journal of Imaging Systems and Technology*, vol. 30, no. 1, pp. 203–215, 2020.

[27] A. Krull, T. O. Buchholz, and F. Jug, "Noise2Void-learning denoising from single noisy images," in *Proceedings of the IEEE/CVF Conference on Computer Vision and Pattern Recognition*. Long Beach, CA: Computer Vision Foundation, June 16–20, 2019, pp. 2129–2137.

[28] W. Wu, M. Chen, Y. Xiang, Y. Zhang, and Y. Yang, "Recent progress in image denoising: A training strategy perspective," *IET Image Processing*, vol. 17, no. 6, pp. 1627–1657, 2023.

[29] N. Rajeswaran, T. S. Lawrence, R. P. Ramkumar, and N. Thangadurai, "An efficient technique to remove Gaussian noise and improve the quality of magnetic resonance image," *International Journal of Innovative Technology and Exploring Engineering (IJITEE)*, vol. 8, no. 10, pp. 2375–2377, 2019.

[30] B. Perumal, R. S. Devi, and M. P. Rajasekaran, "Extermination methods of image noises: A review," *3C Tecnología: Glosas de Innovación Aplicadas a la Pyme*, no. Special Issue, pp. 243–259, 2021.

[31] B. Nisha and M. V. Jose, "DTMF: Decision-based Trimmed Multimode approach Filter for denoising MRI images," *Soft Computing*, vol. 28, no. 7, pp. 6327–6342, 2024.

[32] X. Wang, Y. Hua, E. Kodirov, D. A. Clifton, and N. M. Robertson, "IMAE for noise-robust learning: Mean absolute error does not treat examples equally and gradient magnitude's variance matters," 2019. [Online]. Available: http://arxiv.org/abs/1903.12141

[33] V. Karpukhin, O. Levy, J. Eisenstein, and M. Ghazvininejad, "Training on synthetic noise improves robustness to natural noise in machine translation," in *Proceedings of the 5th Workshop on Noisy User-generated Text (W-NUT 2019)*. Hong Kong, China: Association for Computational Linguistics, 2019, pp. 42–47.

[34] O. Grigas, R. Damaševičius, and R. Maskeliūnas, "Positive effect of super-resolved structural magnetic resonance imaging for mild cognitive impairment detection," *Brain Sciences*, vol. 14, no. 4, pp. 1–26, 2024.

[35] R. Halim and G. Putra Kusuma, "Enhancing image clarity with the combined use of REDNet and attention channel module," *International Journal of Computing and Digital Systems*, vol. 16, no. 1, pp. 213–223, 2024.

[36] L. Kong, Z. Li, Y. Liu, J. Zhang, M. Chen, Q. Zhou, X. Qi, X. W. Deng, and Y. Peng, "A generalized deep learning method for synthetic ct generation," *International Journal of Radiation Oncology, Biology, Physics*, vol. 117, no. 2, 2023.

[37] P. Batarius, A. A. Sinlae, and E. F. Fahik, "Anal-

ysis of the quality of natural dyes in weaving exposed to sunlight using MSE and PSNR parameters," *Jurnal RESTI (Rekayasa Sistem dan Teknologi Informasi)*, vol. 6, no. 5, pp. 797–802, 2022.

[38] Y. Y. Al-Aboosi, R. S. Issa, and A. K. Jassim, "Image denosing in underwater acoustic noise using discrete wavelet transform with different noise level estimation," *TELKOMNIKA (Telecommunication Computing Electronics and Control)*, vol. 18, no. 3, pp. 1439–1446, 2020.